Systems & Control Transactions

Research Article
Foundations of Computer Aided Process Design (FOCAPD 2024)
Breckenridge, Colorado, USA. July 14-18, 2024
Peer Reviewed Conference Proceeding

PSE PRESS

Design and Optimization of Processes for Recovering Rare Earth Elements from End-of-Life Hard Disk Drives

Chris Laliwala, Ana I. Torres*

Carnegie Mellon University, Department of Chemical Engineering, Pittsburgh, PA, USA.
* Corresponding Author: aitorres@cmu.edu.

ABSTRACT

As the United States continues efforts to decarbonize the power and transportation sectors, significant challenges associated with the reliance of clean energy technologies on rare earth elements (REEs) will have to be overcome. One potential approach for increasing the supply of these elements is to extract REEs from end-of-life (EOL) hard disk drives (HDDs). HDDs contain neodymium and praseodymium, which are among the most important REEs for the clean energy transition, as they are crucial to producing the permanent magnets needed for wind turbines and electric vehicles. Here, we propose a superstructure-based approach to find the optimal pathway for recovering REEs from EOL HDDs. The superstructure was optimized by maximizing the net present value (NPV) over 15 years. Projected prices for commercial rare earth oxides and the projected amount of EOL HDDs in the U.S. were estimated and used in the model. These projections were used to establish the base case optimal result, assuming that the plant recycles 60% of personal computers EOL HDDs in the U.S. each year. The model was then expanded to consider the recycling of EOL HDDs generated before the beginning of plant production. Next, a sensitivity analysis was conducted to evaluate the impact of different parameters on the venture's profitability and the optimal processing pathway. Combined, these results offer both valuable insights into the economic viability of REE recycling extraction and a method for performing similar analyses in the future.

Keywords: Recycling, Rare Earth Elements, Process Design and Optimization.

INTRODUCTION

The climate crisis presents one of the most significant challenges facing humanity in the twenty-first century, as the Earth has already exceeded pre-industrial temperatures by 1.1°C [1]. It is imperative to take immediate action to prevent further temperature increases, with a preference for staying within 1.5°C above pre-industrial levels [1]. This requires giving priority to the decarbonization of energy and our economy, including a transition to clean energy technologies such as solar panels, wind turbines, and electric vehicles to reduce emissions in the power and transportation sectors. Notably, in the United States, substantial legislative efforts, such as the "Bipartisan Infrastructure Law," entail an unprecedented investment of more than $430 billion by 2031, aimed at decarbonizing energy among other initiatives [2].

Electrification initiatives are heavily dependent on rare earth elements (REEs). Presently, the United States mines approximately 15% of the world's REEs but exports all raw materials for separation and refinement, primarily to China, which is responsible for mining around 60% of the world's REEs and maintains near-monopoly control over the entire supply chain [3]. This dependency represents a risk to domestic decarbonization efforts, primarily in terms of establishing domestic supply chains to produce clean energy technologies. Therefore, it is vital for the United States to strengthen its domestic rare earth supply chain as it embarks on the journey toward decarbonization.

The objective of this work is to create an optimization-based framework for designing the most efficient processing pathway for recovering rare earth elements from end-of-life hard disk drives (EOL HDDs). HDDs have received increasing attention in the U.S. as a potential source for REEs as evidenced by the work of agencies and

national laboratories (see for example NREL, EPA, and CMI webpages) [4-6]. The paper is organized as follows; first, an estimation was made regarding the projected quantity of REEs available for recycling from EOL HDDs over a period ranging from 2014 through 2038 [7-13], along with a projection of rare earth oxide (REO) prices over the plant's operational lifetime [14]. Next, a superstructure was formulated containing all potential processing pathways for recovering rare earth elements as rare earth oxides from the incoming HDD-based feedstock. Finally, optimization techniques were employed to find the processing pathway that maximizes the net present value over a 15-year period.

MODEL ASSUMPTIONS

Rare earth elements (REEs), which encompass the lanthanide elements, scandium, and yttrium, are categorized into two groups based on their atomic weight: light rare earths (LREs) and heavy rare earths (HREs). LREs comprise Ce, La, Pr, Nd, and Sm, while HREs encompass Eu, Gd, Tb, Dy, Ho, Er, Tm, Yb, and Lt. These elements serve various purposes, with magnets (Nd, Pr, Dy, Sm) constituting 29% of their usage, catalysts (La, Ce) contributing to 20%, and polishing agents (La, Ce) making up 13% across the top three global end-use sectors [15]. The varying abundance of individual REEs within deposits results in some elements being in surplus globally while others face shortages. Consequently, their prices exhibit significant discrepancies, with Nd/Pr being almost 100 times more valuable than La and Ce [15, 16]. HDDs contain relatively large amounts of Nd/Pr.

Two scenarios were examined in this paper. For the first scenario, only EOL HDDs generated during the plant's operational phase were considered. In this scenario, we assumed that 60% of all available EOL HDDs in the U.S. each year would be recycled and available to the plant [8]. In the second scenario, the model was expanded to consider the EOL HDDs generated in the U.S. prior to the start of production. In this scenario, it was assumed that 25% of all EOL HDDs generated in the U.S. over the period ranging from 2014 to 2024 would be recycled by the plant in addition to recycling 60% of all EOL HDDs available in the U.S. each year. For both scenarios, it was assumed that the plant's construction would begin in 2024 and be completed by 2025, after which production would start and continue for 14 years through 2038.

Several sources were used to estimate and quantify the amount of feedstock available for recycling as detailed in the subsequent section [7-13]. To estimate the price of the neodymium oxide, the rare earth oxide (REO) product of this process, over the operational lifetime of the plant, projections were taken from [14] and extrapolated through 2038.

We assumed HDDs to have a lifetime of 8 years [8]. The composition by wt. % of the average HDD rare earth permanent magnets (REPM) is 30 wt. % Nd/Pr, 66 wt. % Fe, and 4 wt. % other (Tb, Dy, Fe, B, Co, or Al) [7]. However, in this analysis, the 'other' category was ignored, and the composition of the REPM was assumed to be 30 wt. % Nd/Pr and 70 wt. % Fe. Note that following currently available data, Nd and Pr were considered together; in what follows Nd should be read as Nd/Pr.

QUANTIFICATION OF FEEDSTOCK AND PRODUCTS

To estimate the amount of REPM available for recycling, the number of EOL HDDs in the U.S. was estimated based on historic and projected sales of laptop and desktop computers in the U.S. and other factors such as HDD type. Although the plant is to run from 2024 through 2038, we wanted to account for all the previously generated EOL HDDs, which we hypothesized some percent of which would still be available for recycling. Thus, the sales of desktops and laptops in the U.S. were estimated over a period of 2006 through 2030.

Sales data for laptops and desktops in the U.S. from 2018 through 2022 was taken from [9, 13]. Additionally, these sources contained projected sales for notebooks and desktops from 2023 through 2028. To estimate sales through 2030, a linear model was fit to the projected sales from 2023 through 2038 and extrapolated through 2038. Estimating sales for years before 2018 proved more difficult due to a lack of data. Thus, the following methodology was employed: First, data for the worldwide sales of personal computers (PCs) and the worldwide sales of laptops from 2006 through 2022 was taken from [10, 11]. Then, the worldwide sales for desktops were calculated by subtracting the sales of notebooks from the sales of PCs. Next, the average percentage of global sales the U.S. accounts for from 2018 through 2022 was calculated. This percentage was assumed to hold from 2006 through 2018. Finally, the annual sales of laptops and desktops in the U.S. from 2006 through 2018 were calculated by multiplying the global sales of desktops and laptops by this percentage.

After estimating the sales of laptops and desktops in the U.S., the next step was to evaluate how many contained HDDs. To accomplish this, we first took data for the global sales of HDDs and SSDs from 2015 through 2022 from [12]. Next, a linear model was fit to the sales data and used to extrapolate sales back to 2006 and up to 2030. In the case of SSDs, this linear model began predicting negative sales in 2012. Thus, the sales of SSDs were assumed to be zero from 2006 through 2012. Using this sales data, the ratio of HDDs to SSDs sold each year was estimated. It was then assumed that this ratio was the same in the U.S. as globally. Additionally, it was assumed to hold for laptops and desktops sold. Thus, the number of HDD-

containing laptops and desktops in the U.S. was estimated by multiplying the sales of laptops and desktops by the percentage of total HDD and SSD sales that HDDs make up. These estimates can be seen in Figure 1.

Finally, using this information, the amount of REPM available for recycling was estimated. HDDs have two sizes: 2.5" and 3.5". We assumed all desktops used 3.5" HDDs and all laptops used 2.5" HDDs. It was also assumed that each 2.5" HDD contains 2.5g of REPM [7]. To estimate the amount of REPM per 3.5" HDD in grams, a linear model taken from [7] was used and shown in Equation 1.

$$17.87 - 0.35t \ (t = 0 @ 1990) \quad (1)$$

Further, it was assumed that the amount of REPM contained within a 3.5" HDD would stop decreasing once it equaled the mass of REPM contained within a 2.5" HDD (2.5g). The annual amount of REPM and Nd available for recycling from EOL HDDs in the U.S. is in Figure 2.

PROCESSES FOR RECOVERING REES FROM EOL HDDS

Rare earth recycling comprises four primary processing stages: disassembly, demagnetization, leaching, and extraction. Each stage contains several potential processes, represented as nodes in Figure 3. The naming convention for the nodes is *<stage number, node number>*, where 1 represents the disassembly stage, 2 the demagnetization stage, 3 the leaching stage, and 4 the extraction stage. The superstructure containing all potential processing pathways can be seen in Figure 3.

For the disassembly stage, three processes were considered: Manual Disassembly *<1,1>*, where REPM is removed from EOL HDDs manually [17]; Automatic Disassembly *<1,2>*, which automates the process with robots [18]; and Shredding *<1,3>*, which involves first heating the HDDs to high temperatures to demagnetize them, after which they are shredded using an industrial shredder. The final node is blank and represents skipping the disassembly stage.

In the demagnetization stage, three processes were explored: Hydrogen Decrepitation *<2,1>*, which involves the reaction of the REPM with hydrogen gas at 170°C for 3 hours to produce a demagnetized, friable material [19]; Heating *<2,2>*, which involves heating the magnets to 350°C for 30 minutes followed by milling [20]; and Extreme Heating *<2,3>*, which involves heating the magnets to 950° C for 15 hours to demagnetize and oxidize them [21] followed by milling. This extreme heating results in

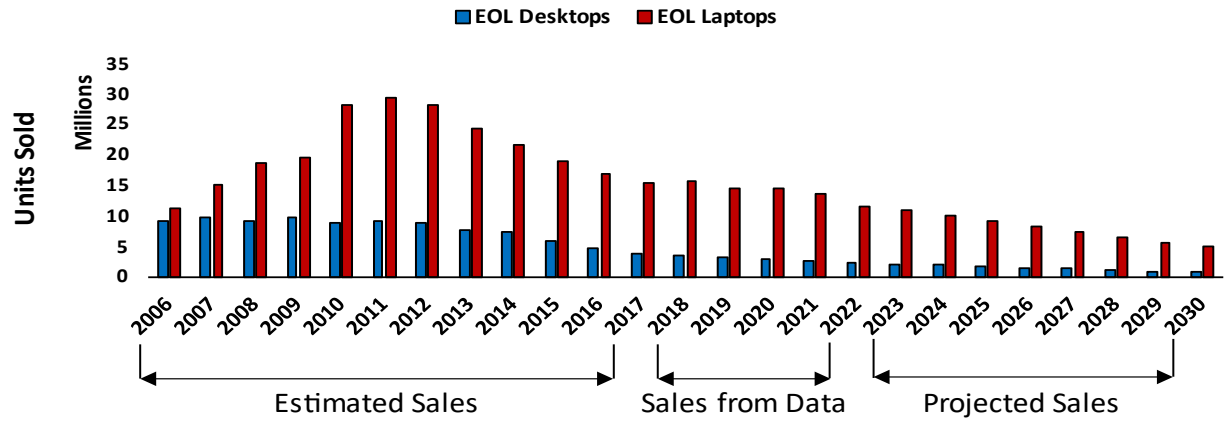

Figure 1: Annual estimated sales, sales from data, and projected sales of desktops and laptops containing HDDs in the U.S. from 2006 through 2030.

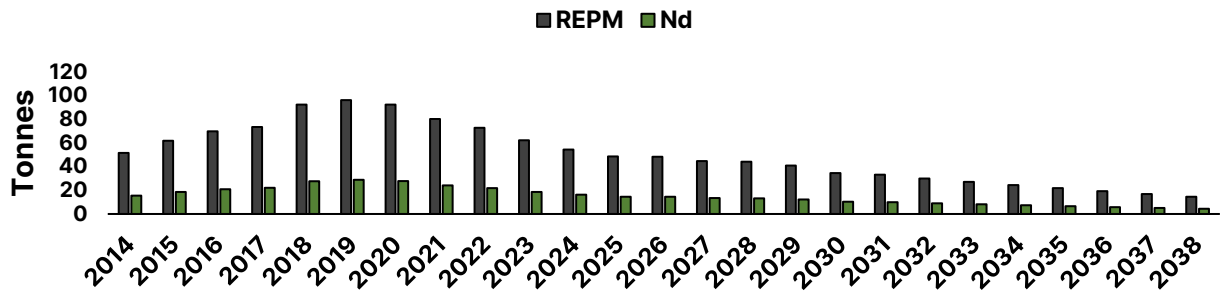

Figure 2: REPM and Nd available for recycling from HDDs in the U.S. from 2014 through 2038.

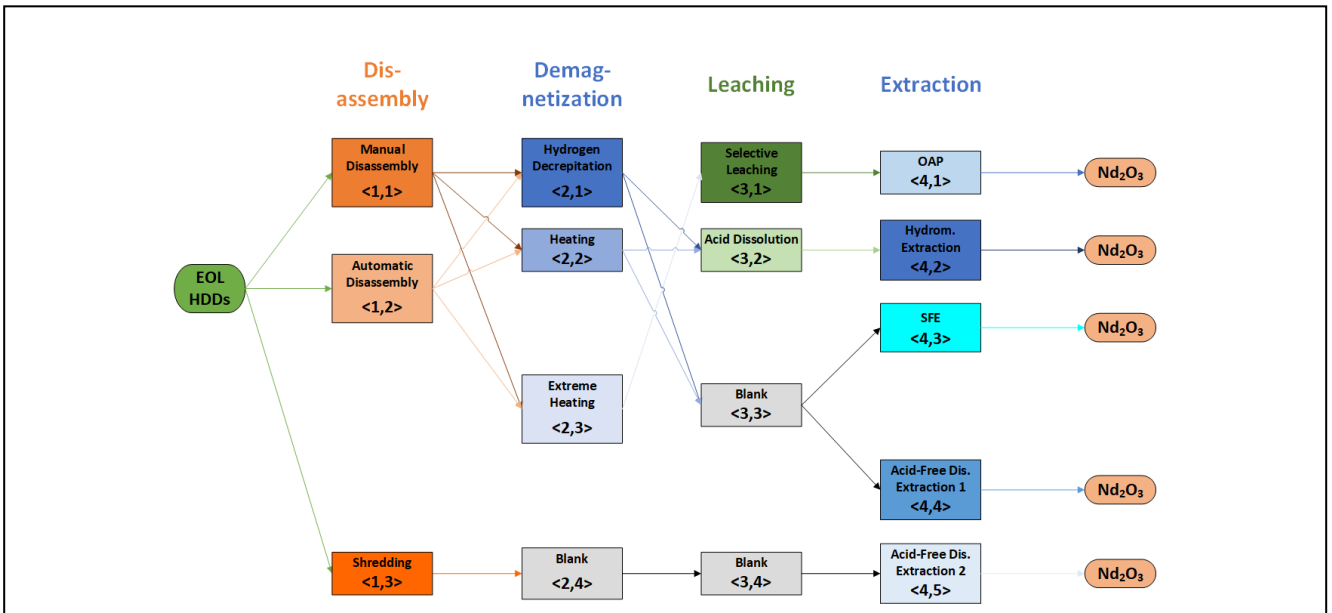

Figure 3: Simplified scheme of the superstructure with processing options for EOL HDDs to REOs.

iron precipitation during the subsequent selective leaching process. The final node *<2,4>* is blank and represents skipping the demagnetization stage.

For the leaching stage, two processes were considered: Selective Leaching *<3,1>* with hydrochloric acid [21], which follows the extreme heating process, and Acid Dissolution *<3,2>* using sulfuric acid [22]. In selective leaching, iron precipitates out of the solution as iron (III) hydroxide. The final two nodes, *<3,3>* and *<3,4>* are blank and represent skipping the leaching stage.

Five processes were examined in the extraction stage. The first process, Oxalic Acid Precipitation (OAP) *<5,1>*, utilizes oxalic acid to directly precipitate neodymium out of solution [23]. The next process, Hydrometallurgical Extraction *<5,2>*, precipitates neodymium as an Nd-sodium double salt to separate it from iron. Subsequent steps involve reactions with oxalic acid and calcination to produce pure Nd_2O_3, with the iron-containing leachate being treated with ammonium sulfate to precipitate it out of solution as iron jarosite [22]. The third potential process, Supercritical Fluid Extraction (SFE) *<5,3>*, utilizes supercritical CO_2 to separate Nd from iron [24, 25].

In the final two processes, Acid-Free Dissolution Extraction 1 *<5,4>* and 2 *<5,5>*, REPM powder is dissolved in an aqueous copper(II) nitrate solution [26]. Next, oxalic acid is added to precipitate neodymium out of solution as neodymium oxalate and iron out of solution as iron-ammonium oxalate. The neodymium oxalate precipitate is then filtered from the soluble iron-ammonium oxalate. Finally, the neodymium oxalate is calcined to produce Nd_2O_3 [26]. These final two processes are identical, except in their final product yield (Nd_2O_3). The yield for this process differs depending on whether the incoming feedstock is shredded HDDs or pure REPM. The yield for a pure REPM feedstock is 98.5 wt. %, while the yield for a shredded HDD feedstock is 73 wt. %. Due to space constraints, details on these processes are not shown in the Figure.

OPTIMIZATION PROBLEM FORMULATION

Equations (2-8) were formulated to describe the superstructure's configuration. A binary variable $y_{i,j}$ is introduced to model the selection of node $< i,j >$. If the node is selected, the binary will equal 1; if not, it will equal 0. Equation (2) enforces that only one node per stage is selected. Equation (3) enforces that if $< 1,1 >$ or $< 1,2 >$ is selected, then either $< 2,1 >$, $< 2,2 >$ or $< 2,3 >$ must be chosen. Equation (4) enforces that if $< 1,3 >$ is selected, $< 2,4 >$, $< 3,4 >$ and $< 4,5 >$ must all be selected. Equation (5) ensures that if $< 2,1 >$ or $< 2,2 >$ are selected, then either $< 3,2 >$ or $< 3,3 >$ must be selected. Equation (6) ensures that if $< 2,3 >$ is selected, then only $< 3,1 >$ or $< 4,1 >$ can be chosen. Equation (7) ensures that if $< 3,2 >$ is selected then $< 4,2 >$ is also chosen. Equation (8) enforces that either $< 4,3 >$ or $< 4,4 >$ is chosen if $< 3,3 >$ is selected. Finally, big-M constraints were added to relate the flow through a unit to its selection, as shown in Equation (9). Here, $F^{in}_{i,j,c,t}$ represents the flow of component c entering node $< i,j >$ in year t, $M^{i,j}$ represents the maximum inlet flow rate for node $< i,j >$, I is the set of all stages in the superstructure, J_i is the set of all nodes in stage i, C is the set of tracked components, and T is the set of all years the plant is in operation. The mass balance for a generic node is illustrated in Figure 4.

$$\sum_{j \in J_i} y_{i,j} = 1 \quad \forall i \in I \tag{2}$$

$$y_{1,1} + y_{1,2} = y_{2,1} + y_{2,2} + y_{2,3} \quad (3)$$

$$y_{1,3} = y_{2,4} = y_{3,4} = y_{4,5} \quad (4)$$

$$y_{2,1} + y_{2,2} = y_{3,2} + y_{3,3} \quad (5)$$

$$y_{2,3} = y_{3,1} = y_{4,1} \quad (6)$$

$$y_{3,2} = y_{4,2} \quad (7)$$

$$y_{3,3} = y_{4,3} + y_{4,4} \quad (8)$$

$$F^{in}_{i,j,c,t} \leq y_{i,j} M^{i,j} \quad i \in I, j \in J_i, c \in C, t \in T \quad (9)$$

Components in the feedstock, intermediates, and products were tracked. The mass balance at each node includes three sequential steps: convergence of the inlet flows from different upstream nodes, processing, and separation of the outlet flows to other downstream nodes. The specific equations are defined in Equations (10-12).

$$\sum_{k=1}^{K^{in}} F^{in}_{i,j,k,c,t} = F^{in}_{i,j,c,t} \quad \forall i \in I, j \in J_i, c \in C, t \in T \quad (10)$$

$$F^{out}_{i,j,c,t} = a_{i,j,c} F^{in}_{i,j,c,t} \quad \forall i \in I, j \in J_i, c \in C, t \in T \quad (11)$$

$$F^{out}_{i,j,c,t} = \sum_{k=1}^{K^{out}} F^{out}_{i,j,k,c,t} \quad \forall i \in I, j \in J_i, c \in C, t \in T \quad (12)$$

Here, $F^{in}_{i,j,c,t}$ is the flow of component c entering node $< i,j >$ in time t, $a_{i,j,c}$ is the yield of component c for node $< i,j >$, $F^{out}_{i,j,c,t}$ is the flow of component c leaving node $< i,j >$ in time t, and $F^{out}_{i,j,c,t}$ is the flow of component c leaving node $< i,j >$ at time t.

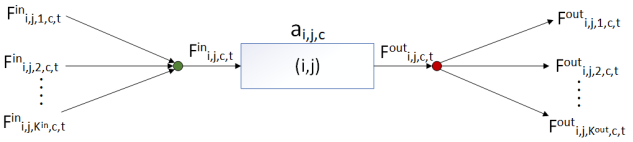

Figure 4: Mass balance framework for generic node $< i,j > \forall c \in C, t \in T$.

ASPEN FLOWSHEETS AND SIMULATIONS

The study and simulation of REE recycling production pathways is a newer and rapidly evolving area of research. Hence, in several cases, process flowsheets with techno-economic analysis were either not available in the literature or the data were of insufficient detail to effectively leverage for this study. Consequently, process flowsheets for several recycling pathways were designed and simulated in Aspen Plus. These flowsheets included the following unit operations: hydrogen decrepitation, heating/high-temperature heating, acid-free dissolution extraction, selective leaching, hydrometallurgical extraction, solvent extraction, and oxalic acid precipitation.

As an example, Figure 5 depicts the Aspen flowsheet designed for the hydrometallurgical extraction process. In the first step, the incoming leachate from the acid dissolution process is reacted with NaOH and ammonium sulfate at a pH of 1.5 to form Nd-sodium double salt precipitates. In the next step, the precipitate is separated from the iron-containing leachate and is reacted with oxalic acid to form neodymium oxalate. The neodymium oxalate is first filtered and then calcined at 750°C in the presence of oxygen to form Nd_2O_3. In the final step, the product is cooled to 100°C using cooling water. However, before the spent leachate can be disposed of, the iron must first be

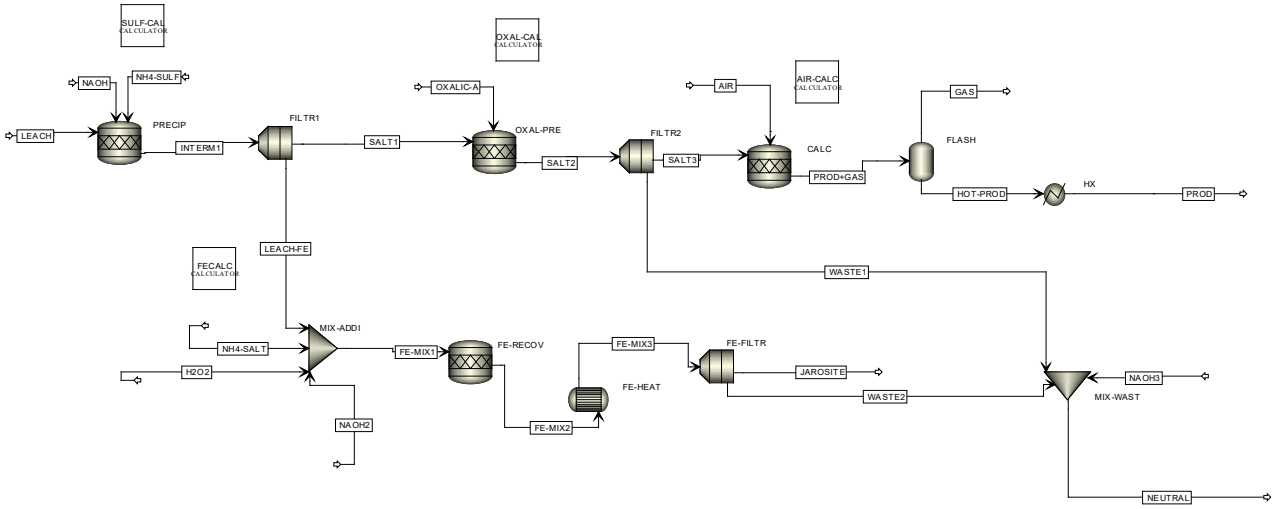

Figure 5: Aspen simulation built for the hydrometallurgical process built using reaction yield data from [24].

precipitated out of solution as jarosite. This is accomplished by heating the leachate to 90°C for 6 hours and reacting it with ammonium sulfate in the presence of an oxidizing agent at a pH of 2 [22]. Finally, the spent leachate is neutralized with NaOH.

The individual operations in these flowsheets were modeled using reaction and separation data from literature. Capital (CAPEX) and operating costs (OPEX) were evaluated using the Aspen Process Economics Analyzer.

OBJECTIVE FUNCTION

The goal of the optimization problem was to maximize the NPV over the plant's lifetime, as shown in Equations (13-14) [27]. Where CF_n is the cash flow in year n, LT is the plant's lifetime in years, and IR is the interest rate.

$$NPV = \sum_{n=1}^{LT} \frac{CF_n}{(1+IR)^n} \tag{13}$$

$$CF_n = Profit_n - (CAPEX_n + OPEX_n) \tag{14}$$

An interest rate of 10% was used as recommended by [28]. Tax and depreciation were ignored. It was assumed that all capital investments were made in year 1, and that the plant does not begin operation until year 2. Therefore, CAPEX was only considered for year 1, after which only profit and OPEX were considered. The methodology described by [27] was used for each node to calculate the CAPEX and OPEX. For OPEX, only the cost of labor was considered for the disassembly stage, and only the cost of raw materials and utilities were considered for the later stages.

Costing information that was available from the literature was adjusted for capacity using a piecewise-linearized approximation of the six-tenths rule [27]. When not available from the literature, Aspen Plus simulations and the Aspen Process Economic Analyzer were used to estimate CAPEX and OPEX costs for a range of flow rates. A linear regression model was then fit to obtain the CAPEX and OPEX vs incoming flow rates.

RESULTS

The optimization problem was coded in Pyomo and solved with CPLEX version 22.1.1.0 using the default options. The decision variables consisted of the operations included in the process and their sizing. The formulation for the MILP optimization problem is as follows:

$$\begin{aligned} \max \quad & z = NPV \\ \text{s.t.} \quad & Eq.(2-12) \\ & F^{in}_{i,j,c,t} \geq 0,\ y_{i,j} \in \{0,1\}\ \forall i \in I, j \in J_i, c \in C, t \in T \end{aligned}$$

The base scenario assumed that the plant recycles 60% of all available EOL HDDs in the U.S. annually [8]. The optimal pathway was found to consist of shredding, followed by acid-free dissolution extraction, and resulted in a negative NPV. The acid-free dissolution extraction processing step was found to be the most significant contributor to CAPEX, accounting for ~90% of the cost. Approximately 162.5 tonnes of Nd_2O_3 were recovered.

Next, we conducted a sensitivity analysis on the percentage of EOL HDDs in the U.S. the plant recycles each year (collection rate, Fig. 6). We found that the plant remained unprofitable even at a 100% collection rate. The NPV breakeven point was found to occur at a collection rate of ~360%, and the optimal process never changed. This suggests that an insufficient number of HDDs are being produced for the plant to leverage economies of scale to be profitable.

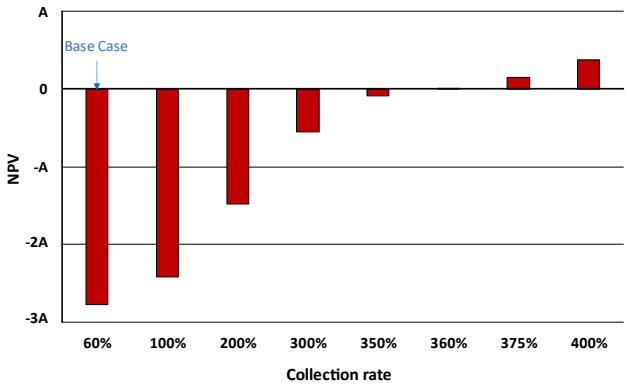

Figure 6: NPV for a varying collection rate. The base case is a collection rate of 60% and no recycling of EOL HDDs generated prior to plant production. The NPV break-even point was found to occur at ~360%. Numerical values are not reported to preserve confidentiality.

Given the results of our first sensitivity analysis, we hypothesized that the optimal process may prove to be profitable when the recycling of EOL HDDs stockpiled from years prior to the beginning of plant production was considered. Therefore, we expanded our model to recycle 25% of all EOL HDDs generated in the U.S. over the period ranging from 2006 to 2024 (initial collection rate) in addition to recycling 60% of all available EOL HDDs each year of operation. The optimal process was found to be the same as that of the previous scenario, however, the NPV was still found to be negative. We then conducted a sensitivity analysis on the initial collection rate and found the NPV breakeven point to occur at ~148% (Fig. 7). The optimal process never changed.

Finally, we conducted a sensitivity analysis on projected REO prices for the expanded model. To vary the projected REO prices, the new projection was assumed to be some percentage of the initial estimate. This percentage was then varied. The NPV breakeven point was found to occur at ~168% of the initial estimate (Fig. 8). Once

again, the optimal process never changed.

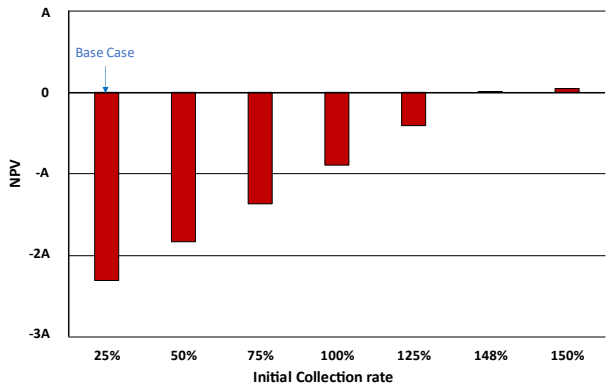

Figure 7: NPV for a varying initial collection rate. The base case has a collection rate of 60% and an initial collection rate of 25%. The NPV break-even point was found to occur at ~148%. Numerical values are not reported to preserve confidentiality.

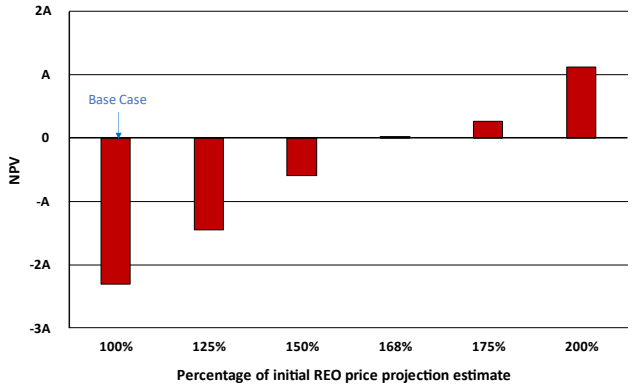

Figure 8: NPV for varying percentages of the initial REO price projection estimate. The NPV break-even point was found to occur at ~168%. Numerical values are not reported to preserve confidentiality.

CONCLUSION

Superstructure optimization was utilized to design a process for the recycling of rare earth elements from EOL HDDs, with the objective of maximizing the NPV. The study determined that the optimal process for both the base case and expanded model consists of shredding, followed by acid-free dissolution extraction. Our results show that the venture considering HDDs from PCs is likely not profitable as a stand-alone plant due to the total amount of REPM available for recycling from EOL HDDs being insufficient given the projected REO prices. However, we hypothesize that by expanding the plant to process multiple feedstocks, or by introducing multiple agents to handle the different processing steps, the optimal pathway may become profitable. Future work will investigate these options.

ACKNOWLEDGMENTS

This effort was funded by the US Department of Energy's Process Optimization and Modeling for Minerals Sustainability (PrOMMiS) Initiative, supported by the Office of Fossil Energy and Carbon Management's Office of Resource Sustainability. Neither the United States Government nor any agency thereof, nor any of its employees, nor the support contractor, nor any of their employees, makes any warranty, express or implied, or assumes any legal liability or responsibility for the accuracy, completeness, or usefulness of any information, apparatus, product, or process disclosed, or represents that its use would not infringe privately owned rights. Reference herein to any specific commercial product, process, or service by trade name, trademark, manufacturer, or otherwise does not necessarily constitute or imply its endorsement, recommendation, or favoring by the United States Government or any agency thereof. The views and opinions of authors expressed herein do not necessarily state or reflect those of the United States Government or any agency thereof.

REFERENCES

1. UNFCCC. https://unfccc.int/documents/310475
2. The White House. https://www.whitehouse.gov/briefing-room/statements-releases/2023/04/20/fact-sheet-president-biden-to-catalyze-global-climate-action-through-the-major-economies-forum-on-energy-and-climate/
3. Oberhaus D, Rare earths for America's future. (2023)
4. NREL. https://www.nrel.gov/news/program/2021/in-a-circular-economy-hard-drives-could-have-multiple-lives-in-the-future.html
5. EPA. https://www.epa.gov/vcs/using-standards-promote-reuse-rare-earth-materials
6. CMI. https://www.ameslab.gov/news/it-s-all-part-of-the-grind-cmi-s-new-hard-drive-shredder-serves-up-plenty-of-material-for#:~:text=The%20Critical%20Materials%20Institute%20specializes,motors%2C%20and%20wind%20turbine%20generators
7. Sprecher B, Kleijn R, Kramer GJ. The case of computer hard disk drives. *Environ Sci Technol* 48, 16:9506-9513 (2014)
8. Maani T, Mathur N, Singh S, Rong C, Sutherland JW, Potential for Nd and Dy recovery from end-of-life products to meet future electric vehicle demand in the U.S. *Procedia CIRP* 98:109-114 (2021)
9. Statista. https://www.statista.com/outlook/cmo/consumer-electronics/computing/desktop-pcs/united-

states?currency=USD&locale=en#revenue
10. Statista. https://www.statista.com/statistics/273495/global-shipments-of-personal-computers-since-2006/
11. Statista. https://www.statista.com/statistics/203691/global-unit-shipments-of-notebooks/
12. Statista. https://www.statista.com/statistics/285474/hdds-and-ssds-in-pcs-global-shipments-2012-2017/
13. Statista. https://www.statista.com/outlook/cmo/consumer-electronics/computing/laptops/united-states
14. Hykawy J, Chudnovsky T. https://www.stormcrow.ca/wp-content/uploads/2021/03/20210308-Stormcrow-UCore-Initiation-Final.pdf.
15. Gielen D, Lyons M. Critical materials for the energy transition: rare earth elements (2021)
16. Smith BJ, Riddle ME, Earlam MR, Iloeje C, Diamond D. Rare earth permanent magnets: supply chain deep dive assessment (2022)
17. Peeters JR, Bracqguene E, Nelen D, Ueberschaar M, Van Acker K, Duflou JR. Forecasting the recycling potential based on waste analysis: a case study for recycling Nd-Fe-B magnets from hard disk drives. *J of Clean Prod* 175:96-108 (2018)
18. Peiró LT, Girón AC, Durany XG. Examining the feasibility of the urban mining of hard disk drives. *J Clean Prod* 248:119-216 (2020)
19. Walton A, Yi H, Rowson NA, Speight JD, Mann VSJ, Sheridan RS, Bradshaw A, Harris IR, Williams AJ. The use of hydrogen to separate and recycle neodymium-iron-boron-type magnets from electronic waste. *J Clean Prod* 104: 236-241 (2015)
20. Klemettinen A, Żak A, Chojnacka I, Matuska S, Leśniewicz A, Wełna M, Adamski Z, Klemettinen L, Rycerz L. Leaching of rare earth elements from NdFeB magnets without mechanical pretreatment by sulfuric (H_2SO_4) and hydrochloric (HCl) acids. *Miner* 11: 1374 (2021)
21. Vander Hoogerstraete T, Blanpain B, Van Gerven T, Binnemans K. From ndfeb magnets towards the rare-earth oxides: a recycling process consuming only oxalic acid. *RSC Adv* 4: 64099-64111 (2014)
22. Lyman JW, Palmer GR. Recycling of rare earth and iron from NdFeB magnet scrap. *High Temp Mater and Process* 11: 175-187 (1993)
23. Nawab A, Yang X, Honaker R. Parametric study and speciation analysis of rare earth precipitation using oxalic acid in a chloride solution system. *Miner Eng* 176: 107352 (2022)
24. Zhang J, Anawati J, Yao Y, Azimi G. Aeriometallurgical extraction of rare earth elements from a NdFeB magnet utilizing supercritical fluids. *ACS Sustain Chem Eng* 6: 16713-16725 (2018)
25. Azimi G, Sauber ME, Zhang J. Technoeconomic analysis of supercritical fluid extraction processes for recycling rare earth elements from neodymium iron boron magnets and fluorescent lamp phosphors. *J Clean Prod* 422: 138526 (2023)
26. Chowdhury NA, Deng S, Jin H, Prodius D, Sutherland JW, Nlebedim IC. Sustainable recycling of rare-earth elements from NdFeB magnet swarf: techno-economic and environmental perspectives. *ACS Sustain Chem Eng* 0: 15915-15924 (2021)
27. Seider WD, Lewin DR, Seader JD, Widagdo S, Gani R, Ng KM. Product and Process Design Principles Synthesis, Analysis and Evaluation. 4th Edition, John Wiley & Sons (2017) ISBN 978-1-119-28263-1
28. Biegler LT, Grossman IE, Westerberg AW. Systematic Methods of Chemical Process Design. Prentice Hall PTR (1997).